

# Optimization of Thin-Film Solar Cells for Lunar Surface Operations

Shawn Breeding\* and William E. Johnson†  
*NASA Marshall Space Flight Center, AL, 35812*

Thin-film solar cells have been in production for decades, but technology has only recently advanced enough to allow for comparable efficiencies to traditional rigid cells. Some of the benefits of thin-films, such as lighter weight and being foldable, are particularly advantageous to space applications since mass and volume are key considerations of any flight project. Using these thin-film cells in space, however, is outside of their ground-based design criteria. This requires special care to be taken in designing the power generation system of a spacecraft around a thin-film solar cell, particularly in regards to thermal management. Without the diffusion of an atmosphere to mitigate solar load, the temperature of the panels can rapidly exceed their design specification. In this paper a design solution is presented that allows for thin-film solar cells to be used in a robotic lunar lander. Due to the low thermal mass and in-plane conductivity of thin films, it is difficult to remove waste heat by any other method than radiation. On the lunar surface this means angling the arrays to increase their view factor to space, which has the negative consequence of decreasing their power generation. An optimization was developed to balance the heat rejection and power generation of the cells, using constraints on the maximum cell temperature and minimum spacecraft power requirements. The resulting solar panel angle was then used as an input to the Thermal Desktop model to verify the final panel temperatures.

## Nomenclature

LPL	=	Lunar Pallet Lander
COTS	=	Commercial Off the Shelf
DFI	=	Development Flight Instruments
a-Si	=	Amorphous Silicon Thin-Film Solar Cell
CdTe	=	Cadmium Telluride Thin-Film Solar Cell
CIGS	=	Copper Indium Gallium Diselenide Thin-Film Solar Cell

---

\*Lead AST, Heat Transfer, Thermal and Mechanical Analysis Branch, NASA MSFC

†Thermal Engineer, Aerodyne Industries

GaA = Gallium Arsenide Thin-Film Solar Cell  
IMM = Inverted Metamorphic Multijunction Thin-Film Solar Cell  
SMU = Source Meter Unit  
 $\epsilon$  = Thermal Emissivity  
 $\alpha$  = Thermal Absorptivity

## I. Introduction

**T**HIN-FILM is a catch-all term for materials with thicknesses on the order of nanometers to micrometers. They can be metals, plastics, or a multilayer combination of the two. They are used extensively in all sorts of products, such as semiconductors, LEDs, and even mirror coatings. The technology to manufacture thin-films is not new, but materials science and manufacturing processes have been steadily improving over the years.[1]

The improvement in materials science and manufacturing is enabling new uses for thin-films that can be of great benefit to the space industry. Thin-film solar cells are of interest due to the mass and cost savings over traditional rigid arrays, but another interesting technology that is being developed is thin-film batteries. [2] Similar to the benefits of thin-film solar cells, these batteries could potentially provide mass and volume savings for spacecraft in the future.

## II. Lunar Pallet Lander Overview

Lunar Pallet Lander (LPL) is a NASA led, medium capacity lander designed to provide payload transportation to the moon. The primary design driver was to keep cost low by using as many commercial off the shelf (COTS) parts as possible and simple structural fabrication. In lieu of traditional spaceflight manufacturing principles, the basic structure is riveted sheet metal. This reduces the need for costly manufacturing techniques, keeping the spacecraft low cost. LPL has been an ongoing development project at Marshall Space Flight Center, in collaboration with several other NASA centers, to develop a low cost landing platform for both fixed payloads and robotic rovers. This is in support of the expanding effort of lunar exploration.

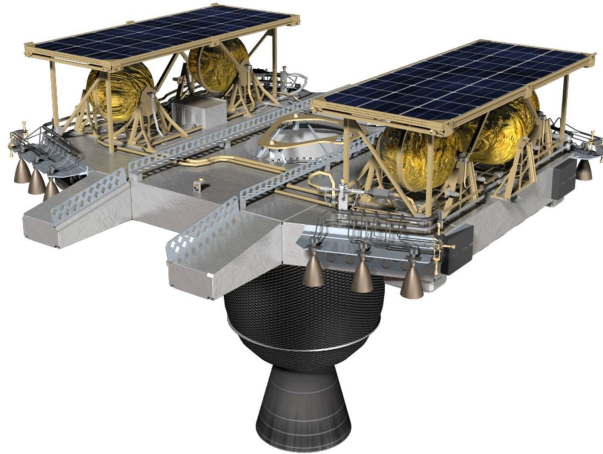


**Fig. 1 LPL Transit Configuration Render**

LPL's predominant feature, as the name implies, is the large amount of open deck space to which payloads can be mounted. Initially the LPL design was rover-centric with ease of access to the lunar surface, but also provides a fixed platform for payload demonstration on the lunar surface. The flexibility provided by simply having open deck space allows for most any payload that fits within the mass and volume constraints. As NASA's most recent plans are to develop a lunar exploration architecture, LPL could support human extensibility by flying Developmental Flight Instrumentation (DFI) packages in order to gain more data about specific landing sights on the lunar surface. The LPL concept can provide quick and simple payload access to the lunar surface with minimal mechanisms.

### **III. Driving Requirement**

The driving requirement for the LPL solar array system is to provide power to the integrated lander and payload from launch vehicle separation until the current end of mission, designated as a full lunar day of illumination. This equates to approximately 336 hours of surface operations.

During this lunar day of surface exposure, power must be made available at various levels for avionics, communications, propulsion safing, heaters, and payloads. At the high latitudes in consideration for LPL (polar regions), there are considerable variations in the solar load due to the lunar horizon, which has large impacts to hardware on the lander system. This environment creates large variations of temperatures across the lander throughout the lunar day, resulting in large variations in heater power needed to maintain hardware temperatures. The solar array system must maintain power availability throughout the lunar day under these conditions.

### **IV. Thin-Film Solar Cells**

Thin-film solar cells are manufactured by depositing a photovoltaic material on top of a substrate, typically a polyimide. Historically they were less efficient than tradition rigid cells due to the photovoltaic materials being used,

but recent advances in materials and manufacturing have made comparable efficiencies possible. Typical thin-film solar cell types are amorphous silicon (a-Si), cadmium telluride (CdTe), and copper indium gallium diselenide (CIGS).[3]

### **A. Design Benefits**

Using thin-film solar cells instead of traditional rigid cells provides several key benefits for space applications. The typical rigid panels used for spacecraft can be costly to procure and require long lead times for mission specific requirements and/or tailoring. With the rigid back-panel and cover glass over the cells, the rigid panels are also quite heavy. By using commercial grade thin-film cells, both cost and mass can be reduced. Recent estimates show that thin-film cells can provide greater than 300% more power per kilogram, while costing less than 50% that of traditional panels. Mass and cost are always driving factors in spacecraft design, so the ability to meet the power requirements at significantly reduced mass and cost are huge advantages.

Another major benefit to using thin films is their ability to be folded compactly. The flexibility inherent in a thin-film allows for clever deployment mechanisms to be designed that can provide for greater mission capability. The increase in capability can be seen at all levels of spacecraft design, from the smallest cubesats to larger landers like LPL. At the cubesat level, a large thin-film solar array can be packed up into a small volume in the cubesat, rather than trying to work a rigid panel into the design. For a lander such as LPL, the customization available by using COTS thin-film cells is an advantage compared to rigid cells.

There are some deployable solar arrays available in industry, but these typically still use rigid panels connected by hinges or other flexible joints. Due to the mass of a traditional panel, the deployment mechanisms also have to be strong and stiff enough to handle vibration loading. On a surface mission, the deployed mass also has to be taken into account since gravity is present. Thin-films do not suffer these issues in their implementation due to their inherently low mass and correspondingly low deployment system mass. Simplistic deployment methods in development for thin-films can consist of flexible booms that roll up similar to a tape measure, with an unrolled deployed configuration.

### **B. Design Issues**

Although there are major benefits to using thin-film solar cells, there are also some downsides. Currently they are only being designed for terrestrial applications, so there is some question about how they will handle the space environment. The primary concerns are radiation exposure and high temperatures decreasing the conversion efficiency of the cell. It is difficult to mitigate the radiation exposure issues by anything other than adjusting flight path to avoid the Van Allen belts, so this paper will not discuss radiation exposure issues other than a small digression in the testing section.

In space the thin-film solar cells receive a higher solar load than they do on the ground, since there is no atmosphere to serve as a diffuser. Additionally, on earth they are subject to natural convection which is not present in space. Both

the higher solar load and inability to reduce the impact of the solar load with natural convection lead to higher cell temperatures in space. Some of the traditional methods used to cool rigid solar panels are ineffective when applied to thin-films, or negate the benefits of using a thin-film. These methods include using a high conductivity backer plate to evenly distribute the heat load and direct it towards a radiator, as well as lowering the panel's packing factor and using a high emissivity ( $\epsilon$ ), low absorptivity ( $\alpha$ ) coating in the space between cells. Neither of these methods work well with the thin-films due to the very low in-plane conductivity of the material.

The exact conductivity is proprietary and has not been measured, but a conservative estimate can be made based on the backer material. The conductivity of a typical polyimide backer material is  $0.20 \frac{\text{W}}{\text{m}^2\text{K}}$ . This inherently low in-plane thermal conduction can be overcome by bonding the cell to a high conductivity back-sheet, as is done with rigid panels, but this negates the ability to fold the thin-film. Adjusting the packing factor is also impractical and would lead to hot-spots forming, since the low conductivity of the film would prohibit the heat from distributing evenly through the material. This is due to the thin-film temperature solely being a function of radiation, which means that the temperature is dictated by the optical properties on both the sun and space viewing surfaces.

### **C. Proposed Design Solution**

Taking the design benefits and issues presented above, a solution to the high temperature problem becomes clear: optimize the array orientation so that the backside has a strong view to space, promoting radiative cooling and greater power generation efficiency. For LPL, the transit portion of the mission was based upon traditional rigid solar arrays and is dictated to operate in a solar inertial orientation to maximize power generation. By deploying a thin-film array system, the solar arrays would have a consistent view to space during power generation and maintain their temperatures via backside radiation. This sets up a balancing act between ensuring the panels can generate enough power while keeping the temperatures within the limits. This is the predominant analysis being presented in this paper.

## **V. Math Model**

Developing a math model is an important step in any analysis, as it allows for a general understanding of the system at hand. This investigation will utilize a simple math model to develop possible configurations, which will then be analyzed further with a more detailed thermal model. The math models also provide validation of the very different methods.

### **A. Simple Math Model**

A simple math model of the transit configuration can be derived from first principles by performing an energy balance, but it is also presented as equation 9.6-15 in [4].

$$T_{op} = \left( \frac{\bar{\alpha}_{Se}}{\bar{\epsilon}_{HF} + \epsilon_{HB}} \frac{S \cos \Gamma}{\sigma} \right)^{\frac{1}{4}} \quad (1)$$

In this equation,  $\bar{\alpha}_{Se}$  is the effective solar absorptance,  $S$  is the solar load,  $\Gamma$  is the angle between the solar cell and the sun,  $\bar{\epsilon}_{HF}$  is the effective front side emittance,  $\epsilon_{HB}$  is the effective back side emittance,  $\sigma$  is the Stefan-Boltzmann constant, and  $T_{op}$  is the absolute operating temperature. The effective solar absorptance and effective front side emittance are described in equations 9.6-3 and 9.6-4 in [4], respectively.

Equation 1 is specifically derived for solar cells and takes into account cell efficiency. It is applicable in the case where the cell is thermally isolated from any conduction into or out of the cell, and the backside has a clear view to space. This makes it applicable for the deployable transit arrays, but not for the surface arrays. This equation provides a steady state temperature prediction and is not mass dependent which is easily seen as applicable to this thin-film system.

## B. Detailed Math Model

Deriving a detailed math model for the lunar surface case is more challenging, as there are more interactions to consider. Unlike the simple math model for the transit case where view factors are readily assumed, the detailed model needs to account for the interaction between the cells, the lunar surface, the sun, space, and other components of the lander (albeit to a lesser extent). At the time of abstract submission, the author believed that a detailed math model would be developed. Project time constraints and the short runtime of the simplified thermal model discussed below resulted in the optimum panel angle being found during the trade study, without the need for a detailed math model.

## C. Power Model

The power generation model can be found as equation 8.6-1 in [4]. A reduced version is shown below in equation 2.

$$P = S' \eta_{conv} F_P F_{EOL} A [1 - F_{PC} (T_{OP} - 25)] \quad (2)$$

In this equation,  $P$  is the power generated,  $S'$  is the effective solar flux,  $F_P$  is the packing factor,  $F_{EOL}$  is an end of life degradation factor,  $A$  is the cell area,  $F_{PC}$  is a power conversion degradation factor, and  $T_{OP}$  is the cell temperature. It can be seen from this equation that as the temperature increases, the power generation decreases.

## VI. Discussion of Thermal Modeling Technique

A model of the thin-film solar cells was created using C&R Technologies (CRTech) Thermal Desktop and incorporated into the integrated LPL thermal model, shown below in figure 2. The cells are modeled as a polyimide film with the optical properties of the solar cells. Since the exact thermal conductivity is unknown, modeling the cell as a polyimide (a lower bound on the thermal conductivity) is a conservative assumption. Surface entities were

used to model the cells, instead of solid entities, and nodes were modeled as arithmetic (zero capacitance). The zero capacitance assumption was made based on lab observations of thin-film temperature changing nearly instantaneously to environment changes. The cells were assumed to have a 100% packing factor, meaning a single optical property on the front side, and were also assumed to be thermally isolated from their frames. Radiative heat transfer was accounted for by using CRTech RadCAD to generate the view factors for the radiation exchange between the cells and space, the sun, and the other components.

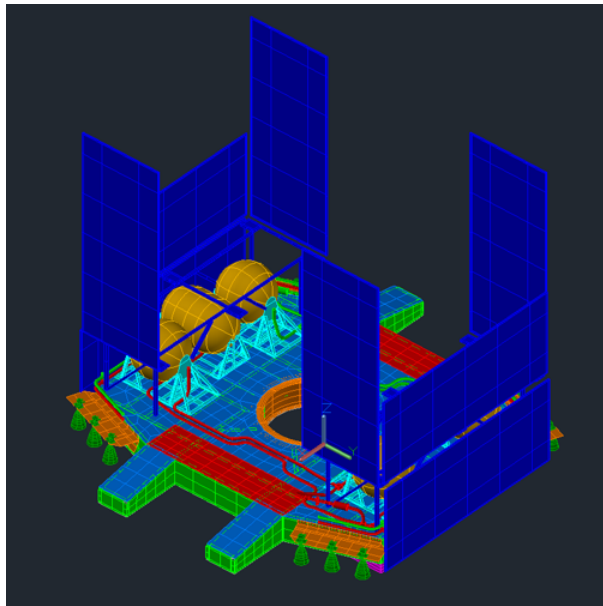


**Fig. 2 Thermal Model of 0° Surface Configuration**

Symbol controlled assemblies were used extensively in order to adjust the angle of the panels. This was important due to the number of configurations being analyzed. Without this parametric ability, multiple copies of the model would have been needed in order to analyze the differences between transit deployed and non-deployed, or the different surface angles. By incorporating the assemblies and using logic inside the symbols, all of the solar panels could be adjusted without causing issues for other cases.

#### **A. Environment Definitions**

There were two main environments that were generated for this analysis: a transit case and a lunar surface case. The transit case models a four day duration with LPL orientated solar inertial with a constant solar load. Since the sun is only in one position during this case, environment calculations and temperature solutions are performed fairly quickly and typically only require 30 minutes of runtime.

The lunar surface case consists of latitude and longitude inputs for the lander location, which must calculate lunar surface environments for 34 different solar loading positions. With the additional details modeled in the LPL integrated

model, this environment calculation and temperature solution can take up to 24 hours of runtime to complete the 14 earth day (approx. 336 hours) transient solution.

### **B. Simplified Thermal Model**

Creating a simplified thermal model was necessary in order to efficiently assess the different solar panel angles. When using a reduced order model, it is important to ensure that the results are accurate to within a small percentage of the full model. Fortunately the solar cells are conductively isolated and the major radiation interactions are with space, the sun, and the lunar surface. Knowing this, a majority of the integrated LPL model components can be removed from the simplified model since they have little impact on the solar cell temperatures.

In order to keep the model intact, it was desired that the reduced order model be contained within the integrated model. Splitting up the models would have ran the risk of updates being made in one not propagating to the other. This functionality was easy to implement by creating a specific radiation group for the simplified model. The only surfaces active in this group were the solar cells, the deck, and the lunar surface. This can be seen in figure 3 below. All the other submodels were inactive, so the processor did not have to calculate the RadKs and fluxes. This model simplification reduced the environment generation and 14 day transient temperature solution time down to less than ten minutes, allowing for rapid trade studies to be performed.

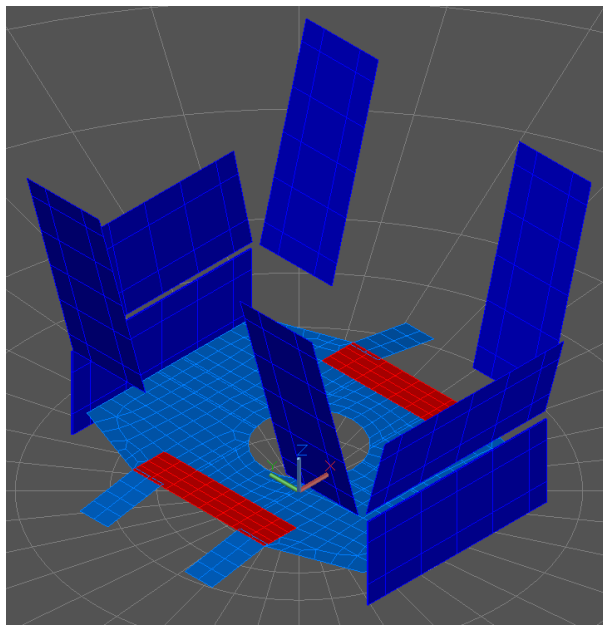


**Fig. 3 Simplified Thermal Model**

## **VII. Modeling Results**

Properties for two types of cells were analyzed in the thermal model: IMM[5] and GaA[6]. Black coating optical properties were used for the backside optical properties of both. The solar cell frontside optical properties are defined as



"active" when the cells are actively generating power and "inactive" when they are not generating power (open circuit) and dealing with the entire environmental load. Based on equation 9.6-3 in [4] an effective absorptivity is used to model the cells under load. This needs to be accounted for due to some of the energy being converted to electrical energy, rather than entirely being converted to heat energy as when the cells are open circuit. Since these cells are designed for terrestrial applications, a target temperature of 60°C is desired to match their design conditions. A summary of the optical properties can be seen below in figure 1.

**Table 1 Optical Property Summary**

Cell Type	$\epsilon$	$\alpha_{\text{active}}$	$\alpha_{\text{inactive}}$
GaA	0.62	0.416	0.616
IMM	0.81	0.617	0.897
Black Coating	0.85	0.90	0.90

The transit case was analyzed with the stowed baseline as shown in the render in figure 1, as well as the deployed configuration shown below in figure 4.

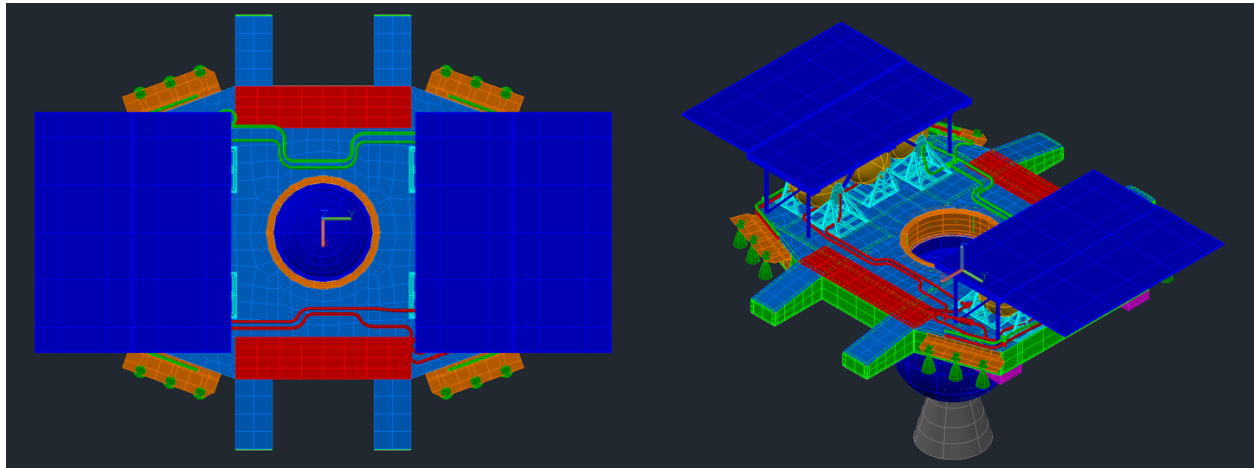


**Fig. 4 Transit Deployed Configuration**

The transit results are summarized in table 2 below. During the transit phase of the mission a maximum power of 630W is required. Power generation during the transit phase is constant, as there is a constant solar load and temperatures reach a steady state value.

**Table 2 Transit Results Summary**

Cell Type	Case	Power Generated (W)	Panel 1 Max Temp (°C)	Panel 2 Max Temp (°C)
IMM	Baseline	835.4	94.1	93.7
IMM	Deployed	907.9	50.5	53.8
GaA	Baseline	613.8	82.4	83.5
GaA	Deployed	641.4	36.3	34.8

Based on these results the IMM cells meet the power requirements in both cases, but only the deployed case meets the temperature target. For the GaA cells, only the deployed configuration meets both the power and temperature target.

The baseline configuration for the lunar surface was panels at 0 degrees (perpendicular to the lunar surface) as shown in figure 2. Additional angles were tested in increments of 15 degrees, up to 45 degrees and 60 degrees for the GaA and IMM cells, respectively. An example of the 30 degree orientation, as well as the panel names, is shown below for the detailed model in figure 5.

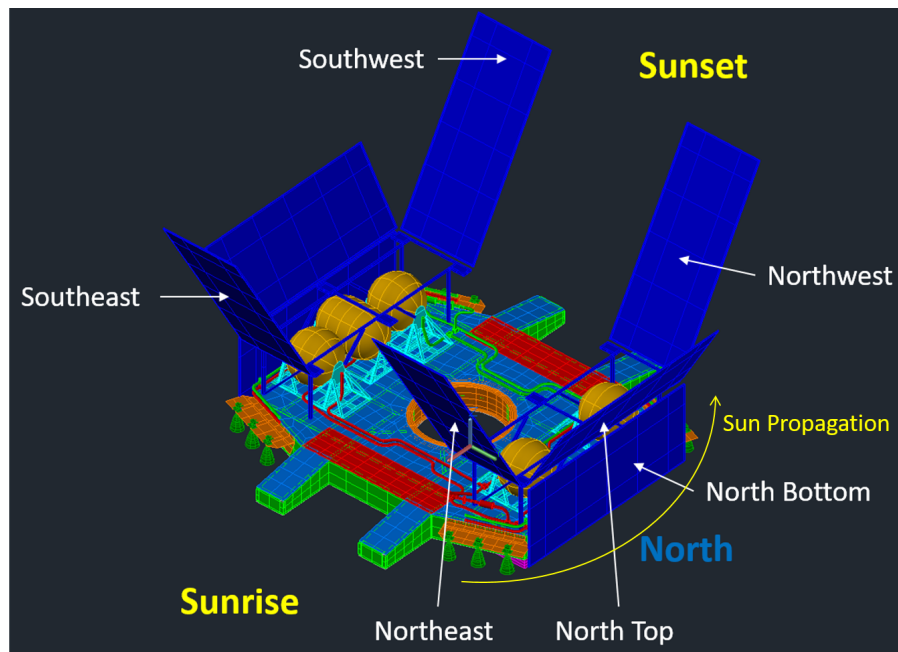


**Fig. 5 Panel Naming Convention**

The results for the IMM cells are below in table 3. All temperatures are the maximum temperatures in degrees Celsius while the cell is under load. The maximum open circuit temperatures were not analyzed. Since the sun moves throughout the lunar day, the power generation is not constant. This leads to a power curve being formed that varies

with time of day, as can be seen for the IMM cells in the baseline 0 degree orientation below in figure 6. The power numbers listed in tables 4 and 3 below are the minimum power that is being generated at this curve. If the minimum power number is above the maximum surface power requirement, then it can be ensured that enough power will be generated throughout the entire lunar surface operations.

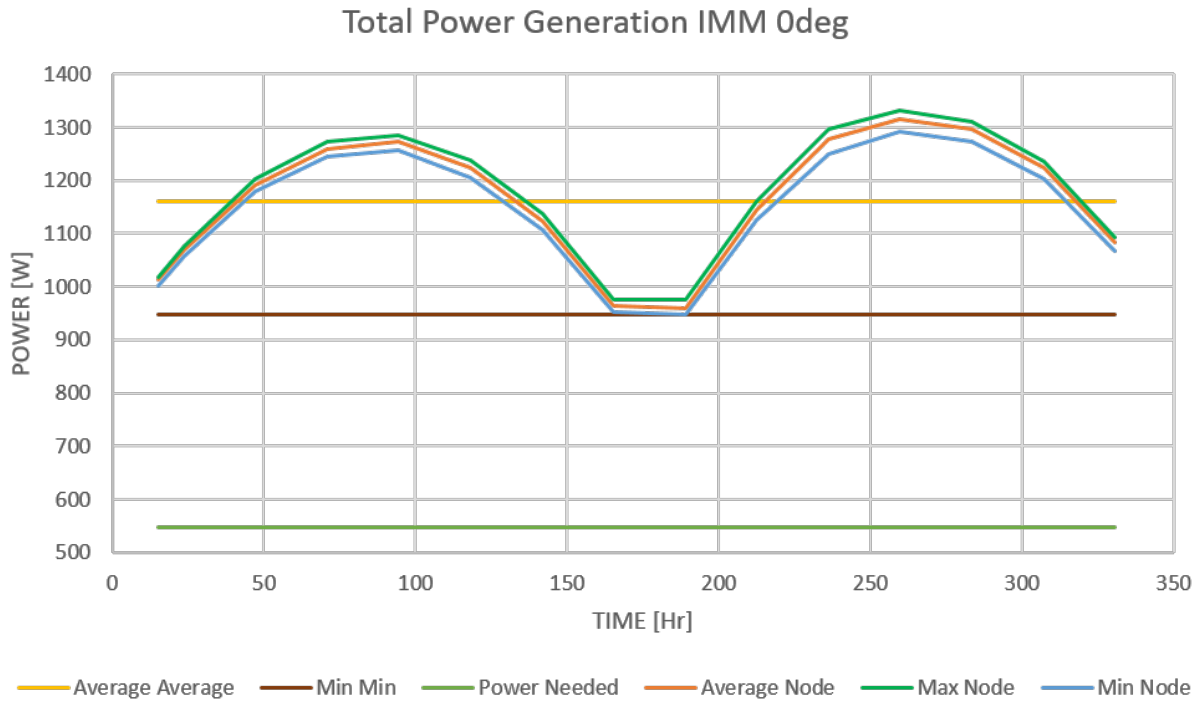


**Fig. 6 Power Curve for IMM 0deg Orientation**

**Table 3 IMM Surface Results**

Case	Power (W)	SE (°C)	NE (°C)	NB (°C)	NT (°C)	NW (°C)	SW (°C)
0deg	962.9	67.5	69.8	72.2	72.2	66.8	69.8
15deg	912.6	61.8	62.0	66.4	66.4	60.7	63.6
30deg	805.5	48.8	51.1	57.0	57.0	48.3	50.6
45deg	641.4	31.1	32.4	45.0	45.0	30.1	33.7
60deg	428.4	4.69	8.25	29.2	29.2	3.59	9.39

During surface operations a maximum of 547W of power generation are needed. Here it can be seen that all the cases except for the 60 degree case meet the power requirements. The 0 and 15 degree cases are borderline on the

temperature requirement. The GaA results are shown below in 4.

**Table 4 GaA Surface Results**

Case	Power (W)	SE (°C)	NE (°C)	NB (°C)	NT (°C)	NW (°C)	SW (°C)
0deg	694.3	53.5	52.6	55.4	55.4	50.1	56.8
15deg	656.6	45.9	44.2	48.1	48.1	42.9	47.5
30deg	575.8	32.1	32.0	38.4	38.4	29.8	33.7
45deg	454.5	14.0	14.7	27.5	27.5	11.8	15.5

Every case except for the 45 degree meets the power requirement with the GaA cells, and all cases are below the 60°C design temperature.

The results above show that there are design solutions that meet the power and temperature requirements, but the specific angle that is chosen will rely on which type of thin-film solar cell is used. Since the IMM cells have a higher absorptivity, they are getting warmer. This is offset, however, by the higher conversion efficiency which means they can tolerate a higher angle and still generate enough power. The GaA cells, on the other hand, are cooler since their absorptivity is lower, but they do not have as high of an efficiency.

## VIII. Thin-Film Solar Cell Testing

An important part of the thin-film solar cell trade study was determining an upper temperature limit. Since the manufacturers only designed the cells for terrestrial applications they did not have good data for the high temperatures that result from direct sun exposure in space. The power conversion becomes less efficient as temperature increases, so it was important to know the temperature at which the cells could no longer meet the minimum power requirements.

### A. Test Apparatus

Three different cell types were tested: IMM, GaA, and CIGS. Coupons with a sample of each cell were made to ensure that all cells were tested under the same test conditions. The coupons were placed in a vacuum chamber so that the only heat transfer would be through radiation, in the same way heat transfer will happen in space and on the lunar surface. In order to mimic the components in the solar spectrum, a solar simulator was used as the light source for the cell's power conversion. A spectrometer was used to measure the light spectrum being emitted by the solar simulator, and minor adjustments were made so that the UV components matched that which the sun produces. A window was present on the front wall of the vacuum chamber to allow the light to shine on the suspended test coupon inside.

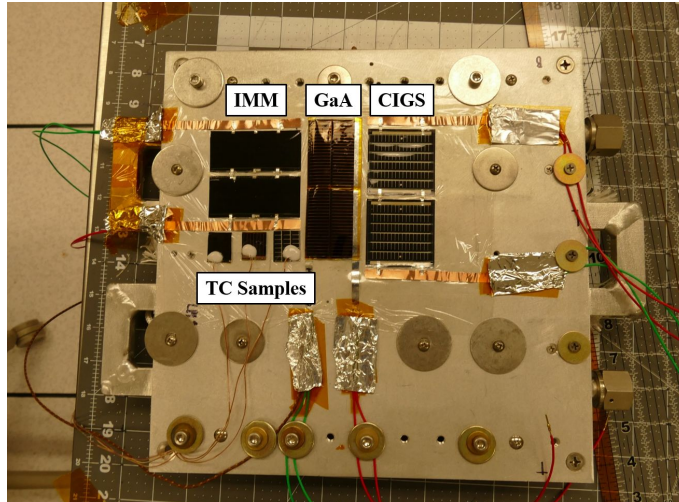


**Fig. 7 Test Coupon**

The test coupons also had a small piece of inactive cell from each manufacturer, to which thermocouples were attached. Thermocouples were also attached on the backing material behind each active cell. The majority of heat needed to reach the target temperature was generated from the solar simulator shining on the samples, but fine temperature control was achieved by using an IR lamp placed behind the test coupon. To measure the power being generated by the cells, a Source Meter Unit (SMU) was used. The SMU was able to serve as a sink for the power being generated by the cells, and was able to measure the voltage and current. This data was recorded and a power curve was generated at the conclusion of each test to show how the power generation decayed over time.



**Fig. 8 Test Coupon in Chamber**

## B. Testing Results

The initial test was run for 213 hours at a an overall average temperature of 140.6°C. The temperature ramp up is shown below in figure 9 and the resulting steady state temperatures in 10.

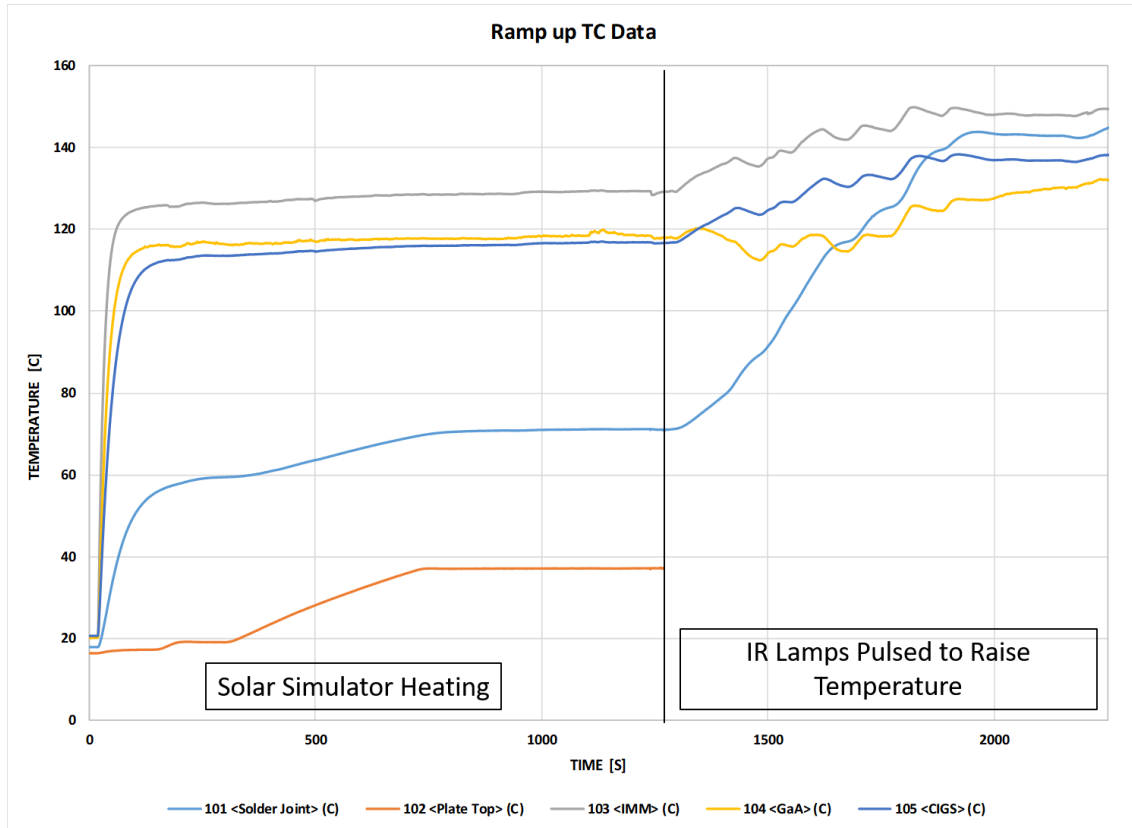
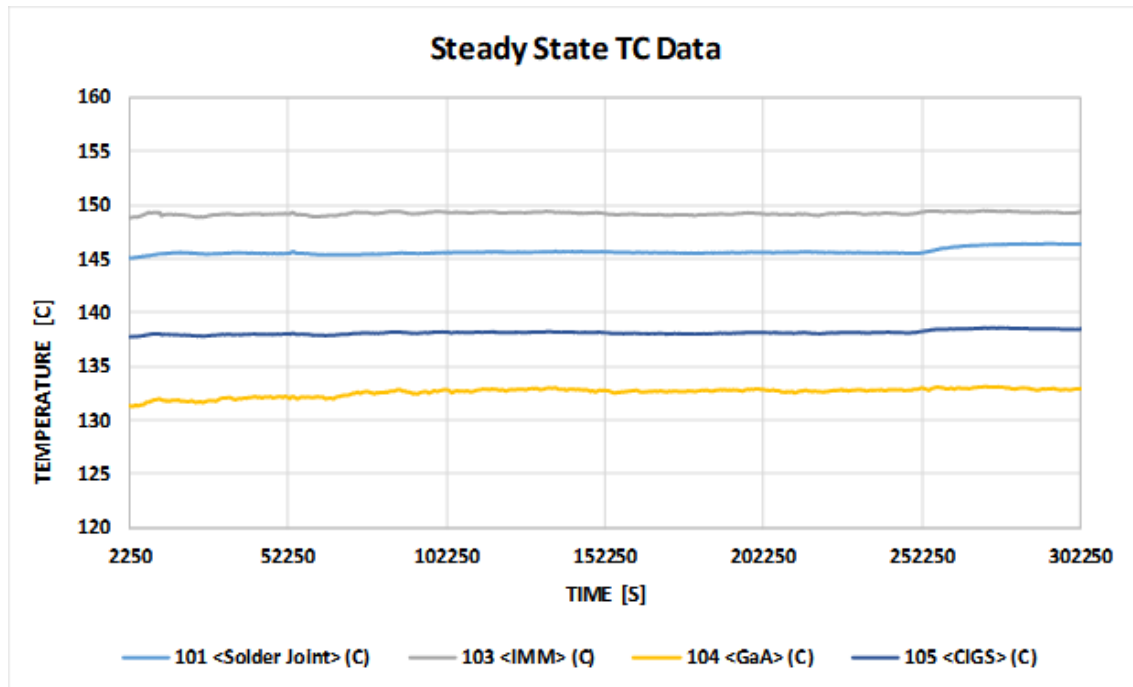


Fig. 9 Test 1 Temperature Ramp Up



**Fig. 10 Test 1 Temperature Steady State**

It can be seen that the heat load from the solar simulator did not heat up the samples to the desired 140°C target temperature. The IR lamps were used to increase the temperature to the target. Results from this test were poorer than expected, and it was unclear initially why this was the case. After some thought it was concluded that the thermocouples measuring the temperatures of the dummy cells were reading lower than the actual cell temperature. To remedy this, thermocouples were taped to the backside of the sample cells. The second test was run using this configuration and results showed that the first test was overtemp by 15-37°C.

Two more tests were conducted using just GaA cells, and the third full coupon is being saved for a final test this fall. During the third test it was noticed that a radiation leak from an adjacent test being run simultaneously in the same building was negatively affecting the results. This can be seen below in figure 11 below. Notice how the degradation is accelerated when there is radiation present. It is unknown how often the radiation was leaking during the previous tests, so those results might be skewed.

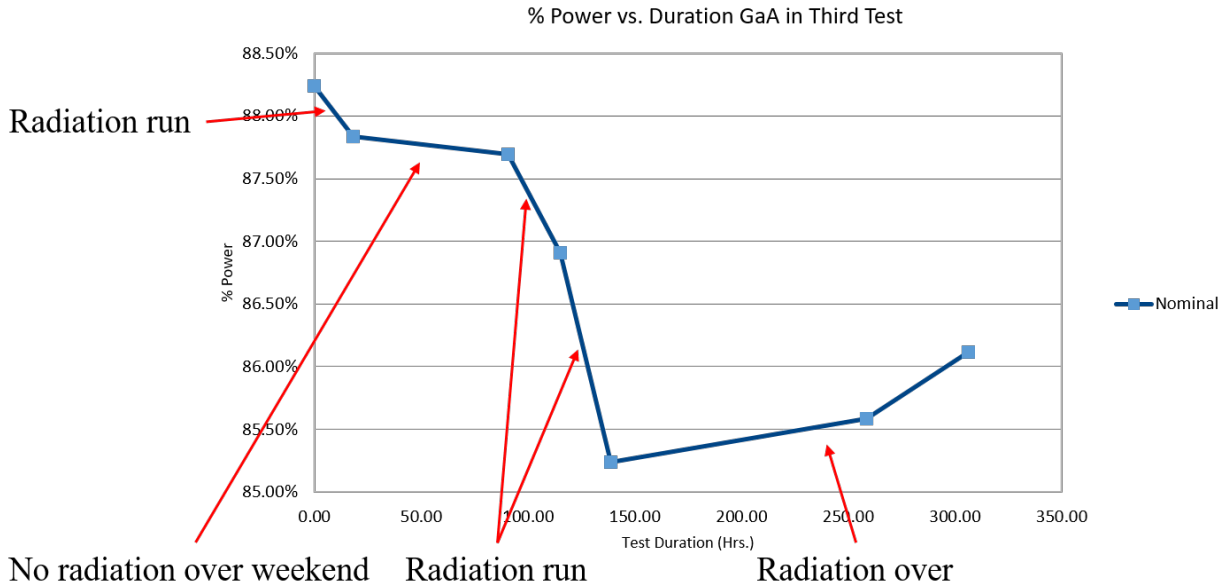


**Fig. 11 Degradation from Radiation Leak**

The fourth test was scheduled to eliminate adjacent radiation sources during testing. The results from this test showed more promise. All the results from the four tests conducted so far are shown in summary table below.

**Table 5 Testing Results Summary**

Test Number	Sample Type	Temperature (°C)	Runtime (Hrs)	EOL Performance	Notes
1	Full Coupon	»140	213	CIGS: 4.2%	[1]
				IMM: 11.5%	
				GaA: 51.2%	
2	Full Coupon	125	76	CIGS: 34.72%	[2]
				IMM: 31.03%	
				GaA: 6.11%	
3	GaA	100-110	306	81.97%	[3]
4	GaA	110-112	168	88.22%	[4]

Notes from test:

- 1) Real temperatures were as high as 180°C.
- 2) Alta shorted out during the test, which is shown by the single-digit EOL efficiency.



- 3) Radiation exposure found from adjacent test, causing accelerated degradation.
- 4) No radiation exposure from adjacent test.

By evolution of the test setup to eliminate temperature and radiation exposure errors, the final test setup will be used along with thermal model predicted behavior to establish a full mission profile test of the thin-film solar cells. This test will simulate the temperatures experienced at each portion of the mission timeline, from the moment the transit solar arrays become active after spacecraft separation to the moment they deploy on the lunar surface. The results of this test will determine if the thin-film cells can survive for the LPL mission.

## IX. Conclusion

Thin-film solar cells are a promising technology for space applications. The benefits of reduced mass and cost are intriguing, along with the ability to easily deploy large panels. Like any new technology, especially a COTS technology not designed for space, there are challenges with utilizing these cells in a spacecraft. Thermally they pose an interesting challenge with a limited amount of solutions. In the trade study presented in this paper, the only feasible solution found was to increase the cell's backside view to space. By doing this it allowed more heat to be radiated to space, which in turn reduces the temperature to a tolerable value. The specific angle is dependent on which cell was chosen due to the different absorption values between the cells.

## Acknowledgements

I would like to thank Dr. John Carr of NASA Marshall Space Flight Center for working with me during this process, and providing the power and testing data.

## References

- [1] Greene, J. E., "Review Article: Tracing the recorded history of thin-film sputter deposition: From the 1800s to 2017," *Journal of Vacuum Science & Technology A*, Vol. 35, No. 05C204, 2017. doi:10.1116/1.4998940.
- [2] Oukassi, S., Giroud-Garampon, C., Poncet, S., and Salot, R., "Ultra-Thin Rechargeable Lithium Ion Batteries on Flexible Polymer: Design, Low Temperature Fabrication and Characterization," *Journal of The Electrochemical Society*, Vol. 164, No. 9, ????
- [3] Ullal, H. S., *Overview and Challenges of Thin Film Solar Electric Technologies*, NREL/CP-520-43355, December 2008.
- [4] Josephs, R. H., *Solar Cell Array Design Handbook*, NASA-CR-149364, October 1976.
- [5] Duda, A., Ward, S., and Young, M., *Inverted Metamorphic Multijunction (IMM) Cell Processing Instructions*, NREL/TP-5200-54049, February 2012.
- [6] Moon, S., Kim, K., Kim, Y., Heo, J., and Lee, J., "Highly Efficient Single-Junction GaAs Thin-Film Solar Cell on Flexible Substrate," *Scientific Reports*, Vol. 6, No. 30107, 2016. doi:10.1038/srep30107.